Pergamon

PII: S0967-0645(96)00049-5

Deep-Sea Research II, Vol. 43, No. 7–8, pp. 1745–1772, 1996

0967-0645/96 $15.00 + 0.00

Effect of small-scale turbulence on feeding rates of larval cod and haddock in stratified water on Georges Bank

R. GREGORY LOUGH* and DAVID G. MOUNTAIN*

(*Received* 13 *October* 1994; *in revised form* 29 *January* 1996; *accepted* 15 *May* 1996)

Abstract—A set of vertically stratified MOCNESS tows made on the southern flank of Georges Bank in spring 1981 and 1983 was analyzed to examine the relationship between larval cod and haddock feeding success and turbulent dissipation in a stratified water column. Observed feeding ratios (mean no. prey larval gut^{-1}) for three size classes of larvae were compared with estimated ingestion rates using the Rothschild and Osborn (*Journal of Plankton Research*, **10**, 1988, 465–474) predator–prey encounter rate model. Simulation of contact rates requires parameter estimates of larval fish and their prey cruising speeds, density of prey, and turbulent velocity of the water column. Turbulent dissipation was estimated from a formulation by James (*Estuarine and Coastal Marine Science*, **5**, 1977, 339–353) incorporating both a wind and tidal component. Larval ingestion rates were based on swallowing probabilities derived from calm-water laboratory observations.

Model-predicted turbulence profiles generally showed that dissipation rates were low to moderate (10^{-11}–10^{-7} W kg^{-1}). Turbulence was minimal at or below the pycnocline ($\approx$25 m) with higher values (1–2 orders of magnitude) near the surface due to wind mixing and at depth due to shear in the tidal current near bottom. In a stratified water column during the day, first-feeding larvae (5–6 mm) were located mostly within or above the pycnocline coincident with their copepod prey (nauplii and copepodites). The 7–8 mm larvae were most abundant within the pycnocline, whereas the 9–10 mm larvae were found within and below the pycnocline. Feeding ratios were relatively low in early morning following darkness when the wind speed was low, but increased by a factor of 2–13 by noon and evening when the wind speed doubled. Comparison of depth-specific feeding ratios with estimated ingestion rates, derived from turbulence-affected contact rates, generally were reasonable after allowing for an average gut evacuation time (4 h), and in many cases the observed and estimated values had similar profiles. However, differences in vertical profiles may be attributed to differential digestion time, pursuit behavior affected by high turbulence, vertical migration of the larger larvae, an optimum light level for feeding, smaller-scale prey patchiness, and the gross estimates of turbulence.

Response-surface estimation of averaged feeding ratios as a function of averaged prey density (0–50 m) with a minimum water-column turbulence value predicted that 5–6 mm larvae have a maximum feeding response at the highest prey densities (> 30 prey l^{-1}) and lower turbulence estimates ($< 10^{-10}$ W kg^{-1}). The 7–8 mm and 9–10 mm larvae also have a maximum feeding response at high prey densities and low turbulence, but it extends to lower prey densities (> 10 prey l^{-1}) as turbulence increases to intermediate levels, clearly showing an interaction effect. In general, maximum feeding ratios occur at low to intermediate levels of turbulence where average prey density is greater than 10–20 prey l^{-1}. Copyright © 1996 Elsevier Science Ltd

INTRODUCTION

Implicit within the dynamics of well-mixed versus stratified waters is the theory of turbulence-related predator–prey contact rates of Rothschild and Osborn (1988). For the

*Northeast Fisheries Science Center, National Marine Fisheries Service, NOAA, Woods Hole, MA 02543, U.S.A.

Arcto-Norwegian cod larvae sampled in the Lofoten, northern Norway, Sundby and Fossum (1990) compared the feeding ratio of recently-hatched larvae with the density of prey (*Calanus finmarchicus* nauplii) and found that contact rate increased by a factor of 2.8 when wind speed increased from 2 to 6 m s^{-1}. Further field data by Sundby *et al.* (1994) showed that the feeding rate of 8–10-day old cod larvae increased by a factor of 7 as the wind speed increased from 2 to 10 m s^{-1}. The fact that feeding rate continued to increase in an area of strong tidal mixing led them to suggest that an optimum feeding level may be found at wind speeds higher than 10 m s^{-1}. Using model simulations for different values of perception distance and reaction time, MacKenzie *et al.* (1994) concluded that an optimum level of turbulence occurred in the mixed layer for wind speeds near 15 m s^{-1}. While contact rates increased with turbulence, the pursuit and swallowing probability depends on turbulence magnitude and larval behavior; that is, ingestion rates for larval fish reach a maximum at intermediate levels of turbulence.

Sundby (1995) further demonstrated that turbulence can influence the feeding rates and survival of larval and juvenile stages up to two months after hatching. In the same study, Sundby did a sensitivity analyses and concluded that the relative change in contact rate was insensitive to the prey's swimming speed, but sensitive to the predator's swimming speed depending on its size and turbulence level. For a first-feeding larva, its sensitivity to swimming speed decreases as turbulence increases; however, for 70-day old juveniles, their greater swimming speed contributes more to the overall contact rate.

Davis *et al.* (1991) examined a series of models on the relationship of turbulence and micropatchiness on growth and recruitment on copepods and fish larvae (haddock). They demonstrated that intermediate levels of wind-induced turbulence (5 m s^{-1}) reduced larval growth by dissipating predator–prey patches, but at higher levels of wind-induced turbulence (> 10 m s^{-1}) growth was restored to the low turbulence levels as a result of the more frequent encounters.

MacKenzie and Leggett's (1991) empirical model simulations evaluated the contribution of wind- and tide-induced small-scale turbulence on encounter rates between larval fish and copepod nauplii. Prey density in relation to larval fish swimming speeds were important parameters in encounter rates. They found that the frequency of contacts between larval fish and their prey could be underestimated by an order of magnitude if one failed to consider the influence of small-scale turbulence when prey density was less than 35 prey l^{-1}.

Neither Sundby and Fossum (1990) nor MacKenzie and Leggett (1991, 1993) consider the vertical profile of turbulent intensity through and below the pycnocline, nor the decrease in tidally generated turbulence away from the bottom. However, the vertical profile of turbulence intensity and its potential effect on prey contact rate could be important in understanding the influence of turbulence on larval fish feeding. Cod and haddock spawned in March–April on northeastern Georges Bank generally are being transported southwest along the southern flank by May when seasonal stratification of the deeper waters (60–100 m) is developing (Lough and Bolz, 1989). Lough (1984) and Lough and Potter (1993) observed that larval haddock and cod were concentrated in the thermocline (pynocline) region, and that their copepod prey also often have higher densities within or above the thermocline (Lough, 1984, Buckley and Lough, 1987). Field observations of suitable prey for larval cod and haddock on the southern flank of Georges Bank in April–May 1981 determined that densities were 5–25 prey l^{-1}, except at a strongly-stratified site where 50 prey l^{-1} were localized at the thermocline between 10 m and 20 m (Lough, 1984). Growth and condition of larvae also were observed by Buckley and Lough (1987) to be better at the

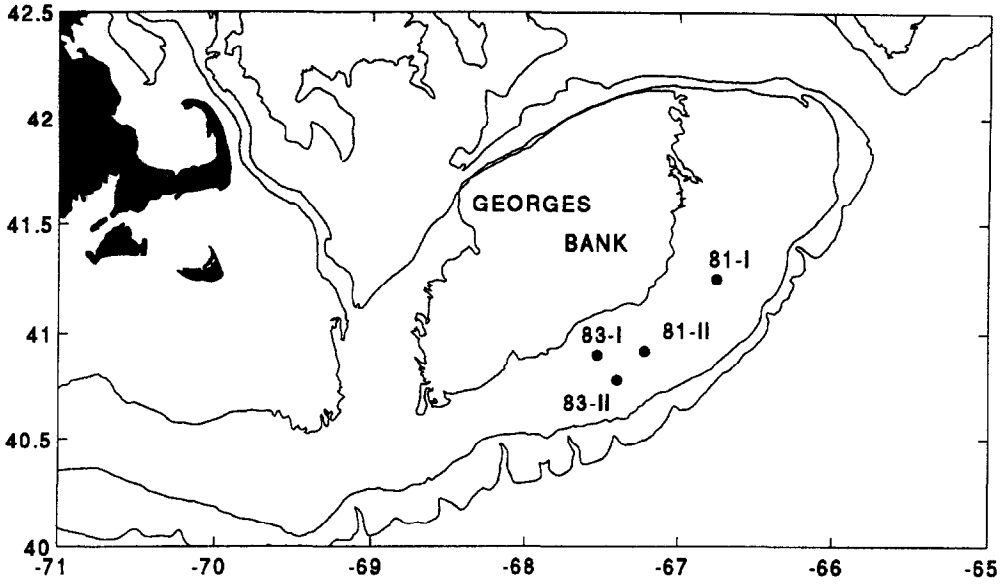

Fig. 1. Map of Georges Bank showing the 1981 and 1983 study sites.

deeper stratified sites than in the adjacent shoal well-mixed waters in May 1983. Herein, we have analysed a set of vertically-stratified tows from the spring of 1981 and 1983 with the view of determining what effect turbulence may have on the feeding rates of three size classes of cod and haddock larvae on Georges Bank.

METHODS

Field sampling and laboratory processing

Cod and haddock larvae and their zooplankton prey were collected on the southern flank of Georges Bank in April and May 1981 and May 1983 (Fig. 1, Table 1). Vertical profiles for fish larvae were made using an electronically-controlled opening/closing net system, a 1-m^2 MOCNESS equipped with nine 0.333-mm mesh nets (Wiebe *et al.*, 1985). For zooplankton

Table 1. *Sampling sites, bottom depth positions, dates and tow numbers for the* 1-m^2 *and* 1/4-m^2 *MOCNESS profiles on the southern flank of Georges Bank in spring of* 1981 *and* 1983

Site	Bottom Depth (m)	Latitude/ Longitude	Sampling Dates	1-m^2 MOCNESS Tow No.	1/4-m^2 MOCNESS Tow No.
81-I	67–70	41 51/66 45	28–29 April 1981	180, 189	179, 181
81-II	75–83	40 55/67 13	21–28 May 1981	191, 193, 199, 205, 207, 220	192, 194, 198, 204, 206
83-I	66–79	40 54/67 32	13–15 May 1983	416, 421, 423, 426	420, 422, 425
83-II	88–93	40 47/67 24	15 May 1983	430, 434, 434	429, 431, 433

prey of larval fish, a 1/4-m^2 MOCNESS with nine 0.064-mm mesh nets was employed (Lough, 1984). Discrete depths were sampled at 10-m intervals from the surface to within 5 m of the bottom. Each net of the 1-m^2 MOCNESS filtered about 250 m^3 of water, and the 1/4-m^2 MOCNESS, about 25 m^3. All net samples were preserved in 4% formaldehyde–seawater solution. Further details of the sampling can be found in Buckley and Lough (1987) and Lough and Potter (1993).

Temperature–salinity profiles were obtained by the MOCNESS sensors and/or CTD and water-bottle samples and averaged over the 10-m sampled strata. Wind speed was obtained from the vessel's bridge log and averaged over five hours prior to the MOCNESS hauls. Only daylight, matching MOCNESS tows (1 and 1/4 m^2) were selected for this study, since larvae are visual feeders and relatively inactive at night (Ellertsen *et al.*, 1980), and station data for these 15 paired tows are listed in Tables 1 and 5.

In the laboratory, fish larvae were removed, their standard lengths measured to the nearest 0.1 mm, and preserved length corrected to live length for shrinkage by the method described in Bolz and Lough (1983). The data were grouped into 1-mm size classes and standardized to number per 100 m^3. Three size classes of cod and haddock larvae were considered in this study: 5–6, 7–8, and 9–10 mm, ranging in age from recently hatched to about 30 days post hatch.

Gut contents of larval cod and haddock were analyzed by dissecting up to 15 specimens of each species from each net sample. Prey remains were identified to the lowest level possible, and their width and length measured to the nearest 0.01 mm by the methods described in Auditore (1984). A feeding ratio, or mean number of prey per larval gut, was calculated for each depth stratum and used as an index of successful feeding activity over the previous four hours (Sundby and Fossum, 1990). Zooplankton from the 1/4-m^2 MOCNESS samples were identified and enumerated by the silhouette photography method described in Lough and Potter (1983). Copepod nauplii that could not be adequately identified to stage or species were grouped. Zooplankton data were standardized to number per liter for each depth stratum.

Prey composition from larval gut contents was used to partition the prey field potentially available to the three size classes of larvae. Larger size prey are generally selected as larvae grow larger (Fig. 2). Since prey are swallowed head first, prey width, corresponding with mouth gape, is considered a more meaningful measurement in assessing the feeding pattern of larval fish than prey length (Hunter, 1981). Prey width size classes of <190, <290, and <450 μm (Fig. 3) correspond with the potential prey field for the larval size classes 5–6, 7–8, and 9–10 mm, respectively. The distribution of the commonly ingested prey items by width size classes is given by developmental stage in Table 2. The 7–8 mm larval prey field would include prey items from both the <190 and <290 μm width classes, and 9–10 mm larval prey field includes prey from all three width classes.

Note that there is no water-column density estimate of *Peridinium* sp. and diatoms, which were found in the smallest larval size class. Also, no *Centropages* spp. were identified in the gut contents, but they can be grouped in the unidentified category. Prey items that may pass through the gut undigested, such as lamellibranch larvae (Tilseth and Ellertsen, 1984), were included since they are relevant to feeding contact rates.

Ivlev curve fit

The relationship between larval feeding ratio and their prey density pooled over all

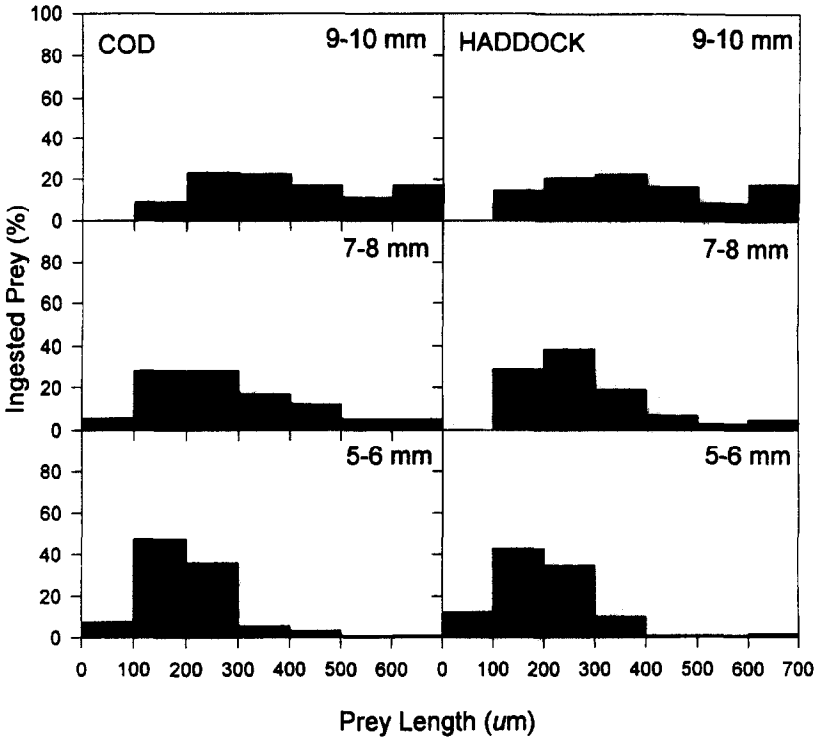

Fig. 2. Frequency of ingested prey by prey length for three size classes of cod and haddock for all specimens combined.

samples was initially examined by the method of Sundby *et al.* (1994) using an Ivlev-type non-linear curve fit

$$FR = FR_{\max}[1 - \exp(-b.PD)],$$

where FR is the feeding ratio (mean no. prey larva^{-1}), $FR_{\max}$ is the maximum feeding ratio, and PD is the prey density (no. l^{-1}) corresponding to larval size class. All depth level data were used for the three size classes of cod and haddock larvae. The coefficient b was estimated using a non-linear regression model in CSS:STATISTICA (StatSoft, 1991). The best curve fit was determined from R^2 values using different values of $FR_{\max}$, which turned out to be 20 for the 5–6 mm size class of larvae and 30 for the 7–8 and 9–10 mm size classes.

Estimating predator–prey contact rates

Simulation of contact rates between predators and their prey according to the theory of Rothschild and Osborn (1988) requires parameter estimates of cruising speeds of larval fish and their prey, the density of prey, and the turbulent velocity of the water column derived from the wind and tide.

Rothschild and Osborn (1988) determined the turbulent velocity in their contact rate formulation from values of the turbulent dissipation rate. Similar to the situation encountered by Sundby and Fossum (1990) and by MacKenzie and Leggett (1991, 1993), the only observations generally available from which to make estimates of the dissipation

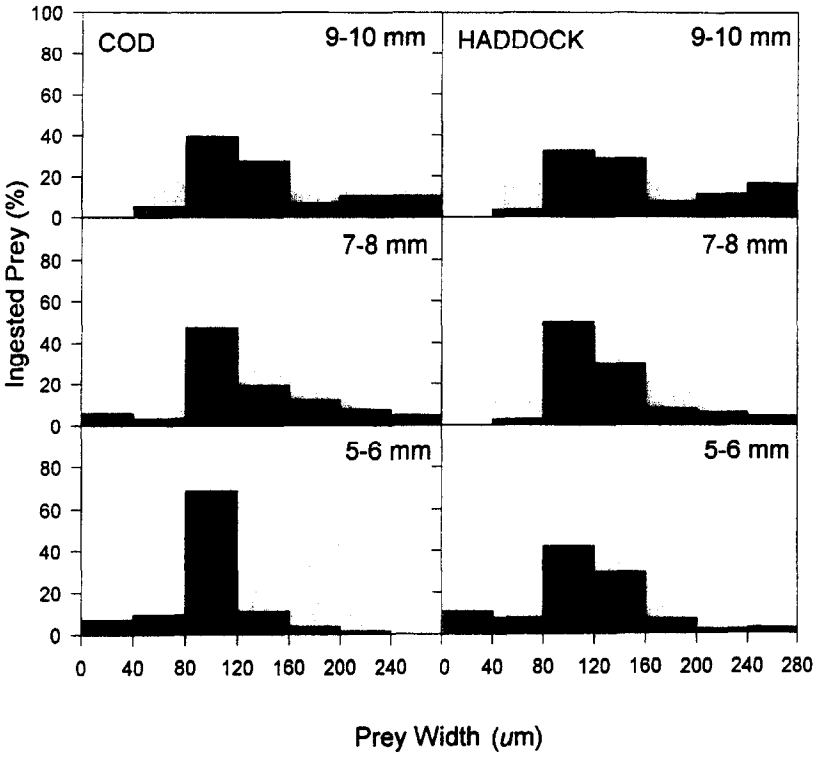

Fig. 3. Frequency of ingested prey by prey width for three size classes of cod and haddock for all specimens combined.

rate are measurements of the water-column temperature and salinity and of the local wind speed. Different from the work of Sundby and Fossum (1990) and MacKenzie and Leggett (1991, 1993), vertical profiles of the dissipation rate in stratified water columns are desired for this analysis.

Table 2. Division of prey items by three width size classes used for estimating the potential prey field from the 1/4-m^2 *MOCNESS samples*

	Width Size Class (μm)		
Taxon	<190	<290	<450
Calanus finmarchicus		CI, CII	CIII, CIV
Centropages typicus	CI, CII, CIII	CIV, CV	A
Pseudocalanus spp.	CI, CII	CIII, CIV, CV	A
Oithona spp.	CI, CII, CIII, CIV	CIV, A	
Copepod nauplii	N		
Copepod eggs	E		
Bivalve larvae		BL	

C = copepodite, A = adult.

The turbulent dissipation rate ε can be parameterized in terms of the vertical shear of the mean current U through use of an eddy coefficient K [Turner, 1981, eqns (8.3) and (8.4)]:

$$\varepsilon = K\left(\frac{dU}{dz}\right)^2,$$

assuming a balance between shear production and dissapation. The eddy coefficient and the vertical shear in the current are estimated through the water column using the formulation in the one-dimensional mixed-layer model of James (1977) (see the Appendix for an explanation of the James formulation). By this method, an estimate of the turbulent dissipation was made at the middle of each depth strata on each MOCNESS tow.

The relative velocity component (V cm s^{-1}) of a larval fish to its prey can be derived from the equation:

$$V = \frac{u^2 + 3v^2 + 4w^2}{3(v^2 + w^2)^{0.5}},$$

where u is the swimming speed of prey (cm s^{-1}), v is the swimming speed of larva (cm s^{-1}), and w is the turbulent velocity (cm s^{-1}). The turbulent velocity term w is given in the notation of MacKenzie and Leggett (1991) as:

$$w^2 = 3.615(\varepsilon r)^{\frac{2}{3}},$$

where ε is the dissipation rate of turbulent kinetic energy (W m^{-3}), and r is the separation distance (m) between predator and prey, here approximated by $N^{-0.333}$ where N is the number of prey per m^3.

Contact rate of the prey, C (prey s^{-1}), is then the relative velocity (V) times the density (D):

$$C = VD,$$

where $D = \pi R^2 N$ and R (cm) is the encounter radius of the predator. Laurence (1985) determined the perception distance for larval haddock as a function of body length (BL) to be 2/3 π (0.75 BL)^2.

A high and low estimate of swimming speed was used for the three size classes of cod and haddock larvae (Table 3). The low estimate was based on a laboratory study of cod larvae by Skiftesvik and Huse (1987), where larvae increased their speed from 0.15 BL s^{-1} at first feeding to 0.25BL s^{-1} at 30 days; i.e. larvae at 10, 20, and 30 days would have swimming speeds of 0.183, 0.217, and 0.250BL s^{-1}, respectively. The high estimate was derived by Miller *et al.* (1988) from a summary of the literature where

$$\log_{(10)}\text{speed(cm s}^{-1}) = 1.07\log_{(10)}\text{length(mm)} - 1.11.$$

Swimming speed of zooplankton prey was based on the estimate of Sundby and Fossum (1990) who used an average speed of 0.5BL s^{-1} for *Calanus finmarchicus* nauplii. Mean length of prey estimated from gut contents in this study increased from about 200 μm for the 5–6 mm size class, to 300 μm for the 7–8 mm, and 400 μm for the 9–10 mm fish (Fig. 2), corresponding to a prey swimming speed of 0.010, 0.014 and 0.020 cm s^{-1} (Table 3).

In order to estimate the original number of prey encountered versus the number of prey captured and swallowed, a swallowing probability (P) was applied based on the empirical equations of Laurence (1985):

Table 3. Parameter estimates for three size classes of larval cod and haddock and their preferred prey used in calculating predator–prey contact rates

	Larval Size Class (mm)					
	Cod			Haddock		
Parameter	5–6	7–8	9–10	5–6	7–8	9–10
Larval mean length (mm)	5.5	7.5	9.5	5.5	7.5	9.5
Age (days post hatch)*	10.8	21.9	30.4	9.2	20.7	29.4
Swallowing probability†	0.34	0.62	0.84	0.32	0.73	0.89
Swimming speed (cm s^{-1})						
Low estimate‡	0.10	0.16	0.24	0.10	0.16	0.24
High estimate§	0.48	0.67	0.86	0.48	0.67	0.86
Prey mean length (mm)	0.205	0.287	0.399	0.198	0.290	0.386
Swimming speed (cm s^{-1})¶	0.010	0.014	0.020	0.010	0.014	0.019

*Bolz and Lough (1988); †Laurence (1985); ‡Skiftesvik and Huse (1987); §Miller *et al.* (1988); ¶Sundby and Fossum (1990).

1. COD $P=0.9(1-0.67\exp(-0.004(W-W_{\min})))$,
2. HADDOCK $P=0.9(1-0.72\exp(-0.0045(W-W_{\min})))$,where W is the larval dry weight in μg and $W_{\min}$ is the minimum larval dry weight in μg. These probabilities give the probability that an encountered prey in calm or turbulent water is actually captured. Length (L) to weight (W) conversions for larvae also are given in Laurence (1985) as

1. COD $W=0.069\,L^{4.049}$,
2. HADDOCK $W=0.042\,L^{4.505}$.

Prey contact rates were estimated for each tow profile using a high and low larval swimming speed. The appropriate swallowing probability was then applied to these encounter rates to determine ingestion rate profiles for comparison with larval feeding ratios.

Response surface estimation

A response surface approach was used to determine an optimum larval feeding rate in relation to prey density and turbulence level. This technique not only provides a predictive model, but also aids visual comparison of the different size classes of larvae (Alderdice, 1972). Multiple regression analysis was applied to the three size classes of cod and haddock feeding ratio data for all depth levels, as well as for feeding ratios averaged over the upper 30, 50, and 70 m of the water column. The mathematical model used in the analysis was of the form:

$$FR = b_0 + b_1(PD) + b_2(TD) + b_3(PD^2) + b_4(TD^2) + b_5(PD \times TD) + e,$$

where FR is the feeding ratio, b_0 is a constant, PD is the linear effect of prey density, TD is the linear effect of turbulent dissipation, PD^2 is the quadratic effect of prey density, TD^2 is the quadratic effect of turbulent dissipation, $PD \times TD$ is the interaction effect between prey density and turbulent dissipation, and e is the error. The multiple regression coefficients and

response surface contour plots were estimated using CSS:STATISTICA (StatSoft, 1991). Given the full functional range of parameters used, one would expect an interaction effect between prey density and turbulence, both positive and negative, since turbulence can enhance contact rates up to some level, beyond which the pursuit process is interrupted.

Larvae and their prey are generally associated with the thermocline region, where turbulence is at a minimum. The minimum turbulence value within each vertical profile was used as a water-column index when prey densities and feeding ratios were averaged over the water column (70–0, 50–0, and 30–0 m). While the largest size class may reside lower in the water column by day and migrate closer to surface at night, the smallest size class of larvae, 5–6 mm, does not vertically migrate and tends to reside more in the upper part of the water column than the larger larvae (Lough and Potter, 1993). Therefore, in one case the turbulence values were averaged over the upper 30 m and used in the response surface analysis.

RESULTS

Larval feeding

The dominant copepods from the Georges Bank samples were *Calanus finmarchicus*, *Pseudocalanus* spp., *Oithona similis*, and *Centropages typicus*, and their life stages comprise the majority of prey items found in the larval guts examined from the 5771 cod and 11,535 haddock (Table 4, Fig. 4). *Pseudocalanus* spp. and *Oithona* spp. were the two most important species in their diet, and the large number of unidentified nauplii and copepodites probably belong to these two species. Their nauplii comprise 20–80% of the prey ingested. More copepodite stages (40–67%) were selected by the largest size class of larvae, 9–10 mm. The phytoplankton prey items *Peridinium* sp. and diatoms were consumed by the smallest, recently-hatched larvae of 5–6 mm, and especially haddock (28%) compared to cod (9%). Copepod eggs ($\sim 120\ \mu m$) in the larval guts accounted for $< 16\%$ of the total prey items and most likely were *Calanus finmarchicus*, which are shed-free. *Pseudocalanus* spp. retain their eggs in sacs until hatched (Corkett and McLaren, 1978), but larvae would have to be large enough to prey on the adult females to ingest them coincidently, and only the 9–10 mm size class of cod and haddock had a small number of adults in their guts.

The smallest nauplii of copepods such as *Oithona* spp. and *Centropages* spp. with carapace lengths of 0.1–0.2 mm, may be extruded through the 0.064-mm mesh to some degree. This bias is probably negligible in the estimation of potential prey field, and less than 17% of the gut contents in this study were in the width size classes smaller than 0.080 mm. Kane's (Kane, 1984) study of larval haddock feeding found that copepod nauplii with widths < 0.070 mm were virtually absent from larval haddock diets.

The plots of larval feeding ratio versus prey density for all depth levels in Figs 5 and 6 show a wide scatter about the non-linear curve fit. High feeding ratios in the range of 20–40 prey larva^{-1} were found at all densites of prey. None of the regressions were significant and explained less than 15% of the variability, thereby supporting previous studies suggesting that small-scale turbulence may be one of several factors that obscure functional relations between larval feeding and prey concentration.

Table 4. Prey items found in gut contents of three size classes of cod and haddock larvae collected by 1-m^2 *MOCNESS tows on Georges Bank, April–May* 1981 *and May* 1983

	Cod						Haddock					
	5–6 mm		7–8 mm		9–10 mm		5–6 mm		7–8 mm		9–10 mm	
Prey items	No.	%	No.	%	No.	%	No.	%	No.	%	No.	%
Phytoplankton												
Peridinium	10	<1	1	<1			95	22.4	134	2.3	1	<1
Diatom	115	7.6	1	<1			25	5.9	3	<1	7	<1
Lamellibranch larvae	99	6.6	39	1.3			20	4.7	128	2.2		
Pteropod	10	<1	22	<1			2	<1	252	4.4	1	<1
Pelecypod							37	8.7				
Copepod eggs	6	<1	167	5.4	60	5.4	67	15.8	154	2.7	877	16.4
nauplii	692	45.8	908	29.3	131	11.7	103	24.3	2341	40.6	816	15.3
copepodites			161	5.2	524	46.8			61	1.1	1524	28.6
Oithona spp.												
nauplii	482	31.9	251	8.1			20	4.7	642	11.1	55	1.0
copepodites	14	<1	296	9.6	84	7.5	1	<1	187	3.2	180	3.4
adults			80	2.6	55	4.9			23	<1	195	3.7
Pseudocalanus spp.												
nauplii	64	4.2	808	26.1	109	9.7	16	3.8	1690	29.3	875	16.4
copepodites			76	2.5	130	11.6			15	<1	396	7.4
adults					2	<1					182	3.4
Calanus finmarchicus												
nauplii	5	<1	259	8.4			5	1.2	88	1.5	143	2.7
copepodites			5	<1	8	0.7			4	<1	22	<1
adults												
Other	14	<1	26	<1	10	1.0	33	7.8	51	<1	61	1.1
Total	1511		3100		1113		424		5773		5335	

Water-column turbulence

The four study sites on the southern flank of Georges Bank had a wide range of turbulence values depending on the depth of the water column, the tidal strength and the wind speed. In April 1981 (Site 81-I), the water column was still in the well-mixed state of winter conditions. In May 1981 (Site 81-II) and 1983 (Sites 83-I and 83-II), varying degrees of water-column stratification had developed due to increased solar insolation and the effect of decreasing winds. Wind speeds ranged from a low of 0.8 m s^{-1} (MOC 199) to a high of 11.2 m s^{-1} (MOC 189). Estimated turbulence profiles for the different MOCNESS tows generally show a minimum at or below the pycnocline, between higher values near the surface due to wind mixing, and at depth due to the large shear in tidal current near the bottom. The minimum value is usually 1–2 orders of magnitude less than the surface and bottom maximum values.

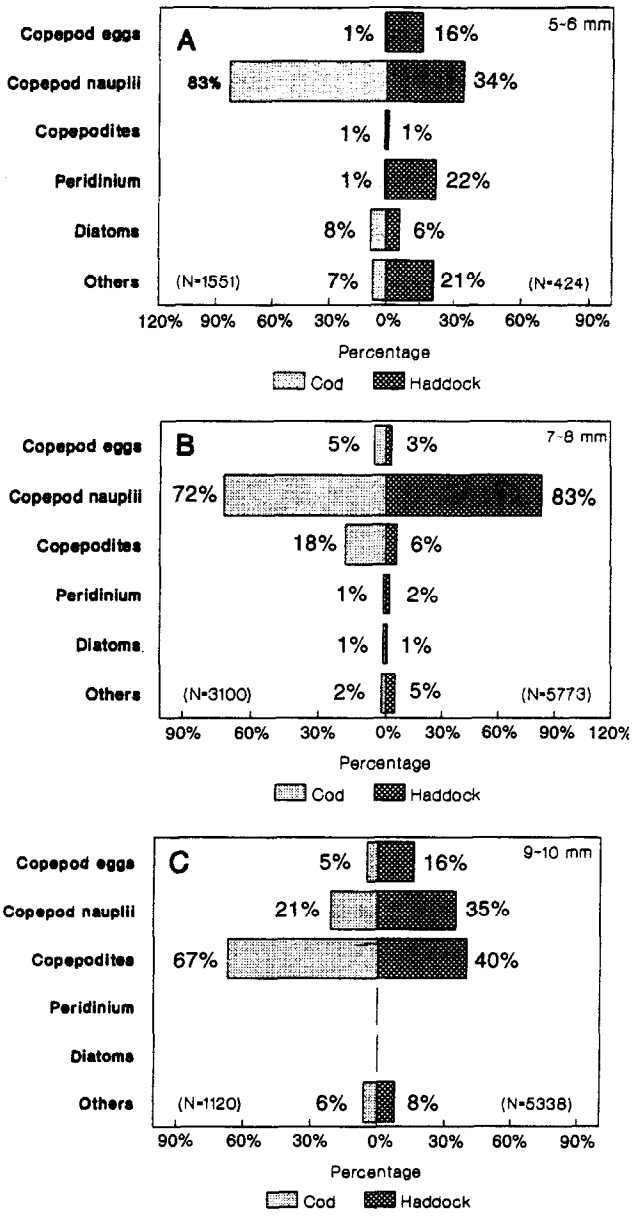

Fig. 4. Percentage prey composition of cod and haddock by three size classes. *N* represents the number of fish guts examined.

Response surface estimation of feeding ratio

Initially, a multiple regression analysis and response surface contour plots were done using all tow stratum values that had the three variables: feeding ratio, prey density, and turbulence estimate, to see if there was a relationship without regard to depth of sample. The multiple regression fit had very low R^2 values ($< 5\%$) so a different approach was taken. If one makes the hypothesis that feeding ratio is related to the degree of stratification, then an index of the water column could be made using the minimum estimated turbulence value.

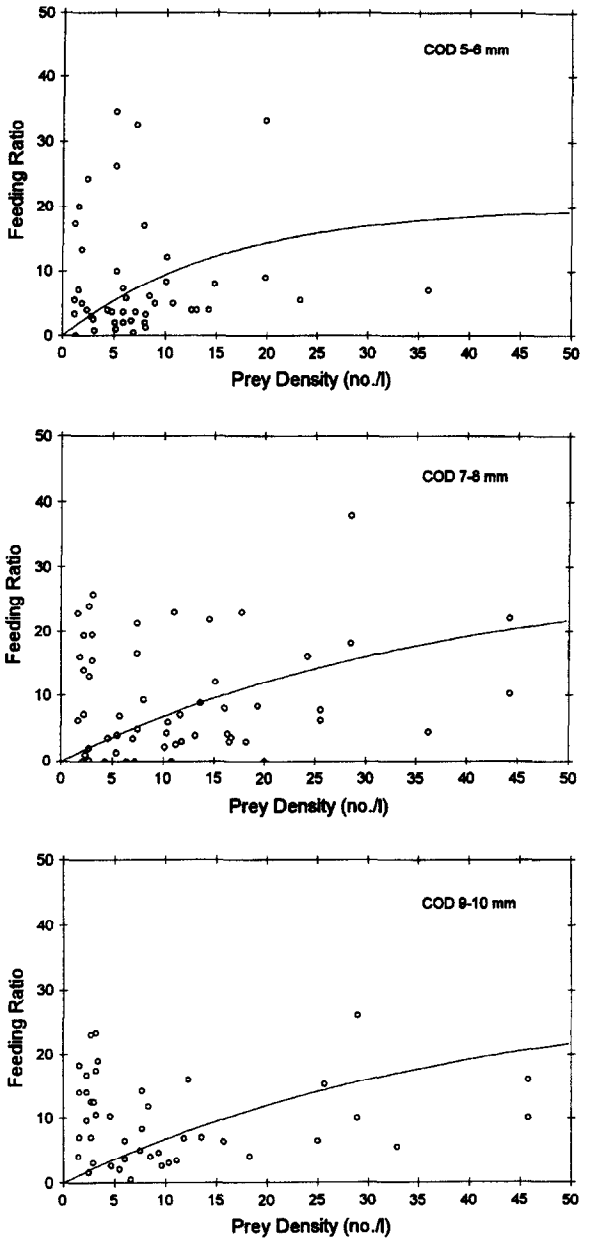

Fig. 5. Feeding ratio versus prey density for three size classes of cod larvae. Each data point represents an individual depth level. The non-linear curve fit used a maximum feeding ratio of 20 for the 5–6 mm size class and 30 for the 7–8 mm and 9–10 mm size classes.

Multiple regressions and response surface contour plots were made using an average water-column value (0–50 m) of feeding ratio versus average water-column prey density (0–50 m) and a minimum turbulence index. Most larvae reside in the upper 50 m of the water column. The MOCNESS tow summary given in Table 5 provides the mean feeding ratio and mean prey density with standard deviations for the three size classes of cod and haddock larvae

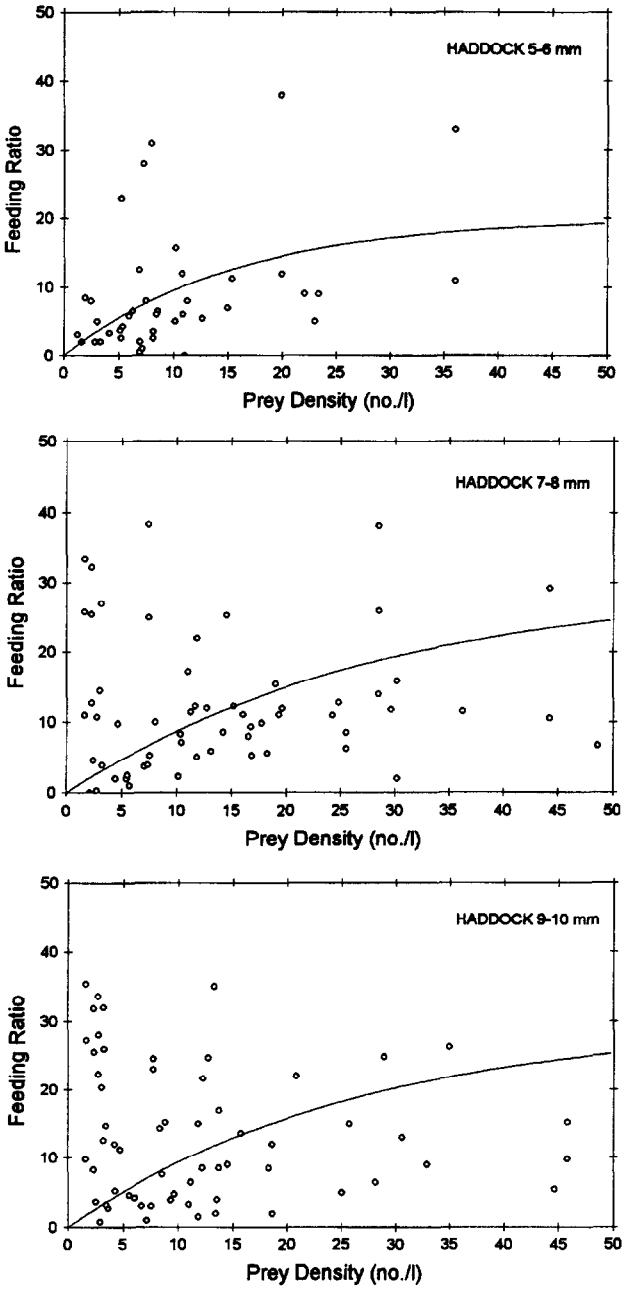

Fig. 6. Feeding ratio versus prey density for three size classes of haddock larvae. Each data point represents an individual depth level. The non-linear curve fit used a maximum feeding ratio of 20 for the 5–6 mm size class and 30 for the 7–8 mm and 9–10 mm size classes.

averaged over the upper 50 m of the water column. The data base consisted of 611 cod and 770 haddock. This analytical approach accounted for more variability in the data; their R^2 values ranged from 32 to 56% (Table 6). In all the regression models, perhaps contrary to

Table 5. Mean feeding ratio (no. prey per larva) and mean prey density (no. prey per liter) for three size classes of cod and haddock larvae averaged over the upper 50-m of the water column. The minimum turbulence value is listed for each tow profile. Vertical profiles of larvae were made by a 1-m² MOCNESS and zooplankton prey by a ¼-m² MOCNESS (haul number in parentheses). See Table 6 for regression model results

	5–6 mm Cod	5–6 mm Haddock	Prey field (<190 μm)	7–8 mm Cod	7–8 mm Haddock	Prey field (<290 μm)	9–10 mm Cod	9–10 mm Haddock	Prey field (<450 μm)	Turbulence
MOCNESS	Feeding ratio $\bar{x}\pm$S.D. (*N*)	Feeding ratio $\bar{x}\pm$S.D. (*N*)	Density $\bar{x}\pm$S.D.	Feeding ratio $\bar{x}\pm$S.D. (*N*)	Feeding ratio $\bar{x}\pm$S.D. (*N*)	Density $\bar{x}\pm$S.D.	Feeding ratio $\bar{x}\pm$S.D. (*N*)	Feeding ratio $\bar{x}\pm$S.D. (*N*)	Density $\bar{x}\pm$S.D.	Minimum rate log (W/kg)
180 (179)	2.3±1.16(3)	2.7±2.39(20)	7.1±4.90	9.7±6.20(0)	0	0	7.8±4.96(6)	0	8.7±6.59	−9.39
189 (181)	6.1±4.66(22)	3.8±4.09(32)	5.5±3.25	8.4±4.35(17)	1.0±0(1)	7.7±4.40	5.0(1)	0	7.1±4.50	−8.85
191 (192)	0	5.4±6.50(5)	22.3±10.21	22.1±12.74(9)	9.9±9.46(23)	31.9±14.25	10.0(1)	8.7±5.95(16)	34.9±11.15	−9.62
193 (194)	0	10.8±5.07(22)	12.4±6.32	0	13.3±6.18(34)	19.3±8.04	0	18.4±13.90(5)	18.9±6.66	−9.19
199 (198)	5.9±4.01(9)	6.0±1.41(2)	9.2±4.64	9.2±5.00(45)	10.7±4.42(42)	16.9±7.71	9.6±4.99(18)	14.4±7.67(28)	14.6±7.38	−10.94
205 (204)	1.9±1.53(27)	3.2±2.62(24)	6.1±1.88	2.6±1.95(18)	5.5±3.89(24)	11.2±5.53	7.0(1)	4.3±2.81(6)	11.4±7.28	−8.99
207 (206)	3.7±3.38(11)	6.5±0.71(2)	8.8±3.42	6.4±3.27(29)	7.7±4.45(30)	15.1±6.29	5.4±3.08(14)	5.5±3.45(28)	13.3±6.73	−9.39
220 (192)	7.0(1)	33.0±45.26(3)	22.3±10.21	16.6±7.89(7)	28.8±17.33(8)	31.9±14.25	16.0±16.97(2)	17.0±8.00(12)	34.9±11.15	−10.48
416 (425)	19.4±9.14(9)	12(1)	6.0±7.95	17.3±6.28(33)	27.5±12.00(18)	8.5±11.43	15.8±9.69(24)	25.6±13.05(51)	8.6±11.58	−9.31
421 (422)	2.7±2.49(23)	5.5±3.32(14)	4.2±3.31	1.8±2.10(35)	4.0±3.45(25)	8.4±7.00	1.9±2.41(7)	2.5±2.03(29)	8.5±6.78	−11.02
423 (425)	5.8±3.78(5)	9.7±7.31(6)	6.0±7.95	6.3±3.73(18)	12.7±7.00(29)	8.5±11.43	8.2±7.33(13)	14.8±10.75(11)	8.6±11.58	−9.83
426 (425)	30.9±11.45(17)	38.0±13.12(3)	6.0±7.95	23.0±14.24(23)	35.0±11.92(31)	8.5±11.43	15.1±6.86(26)	32.4±9.51(28)	8.6±11.58	−9.68
430 (429)	3.7±2.09(27)	6.0±2.50(9)	6.5±3.05	3.2±0.45(10)	4.7±3.94(21)	8.4±4.52	3.3±1.16(3)	3.7±1.60(32)	8.5±4.66	−10.81
432 (431)	9.1±5.33(30)	9.0±5.27(10)	10.2±7.83	6.1±5.67(16)	10.2±4.53(42)	18.9±11.29	3.7±2.45(10)	10.2±2.28(12)	16.6±10.28	−10.97
434 (433)	29.1±9.32(16)	29.5±2.12(2)	4.3±3.02	22.3±9.58(18)	21.4±8.17(21)	7.1±5.31	15.4±3.95(7)	19.7±8.45(18)	7.1±4.91	−9.84

Table 6. Multiple regression parameter estimates for larval cod and haddock feeding response in relation to average prey density and minimum turbulent dissipation in the upper 50 m of the water column

Larvae	Size Class (mm)	Parameter Estimates						
		Constant	PD	TD	PD^2	TD^2	PD × TD	R^2
Cod	5–6	−1281.740	−57.508	−292.842	0.056	−16.002	−5.250	0.563
	7–8	−691.217	−6.553	−147.714	0.036	−7.621	−0.522	0.534
	9–10	−459.807	−6.168	−99.856	0.012	−5.238	−5.560	0.478
Haddock	5–6	−1408.280	−17.763	−290.961	0.018	−14.783	−1.700	0.458
	7–8	−1623.260	−10.125	−335.190	−0.027	−17.113	−1.093	0.546
	9–10	−829.479	−7.581	−177.327	−0.022	−9.281	−0.817	0.317

PD = prey density, TD = turbulent dissipation.

expectations, there are negative relations between feeding ratio and the parameters of averaged prey density and the turbulence index. Significance of the parameter estimates is not important here because of the exploratory nature of the approach, and because there are limited data sets to make a rigorous predictive model. The model does permit one to see where the optimum feeding response lies in parameter space and how it is oriented. Feeding ratio contour plots are shown for the three size classes of haddock in Fig. 7; plots for cod are not shown. The orientation of the contours as saddles shows the interaction effect of prey density and turbulence; i.e. there is a ridge effect in feeding response over the independent variables. For 5–6 mm haddock, the highest feeding ratio occurred at the highest prey densities (> 30 prey l^{-1}) and lower turbulence levels ($< 10^{-10}$ W kg^{-1}). For the 7–8 mm size class, the maximum feeding ratio observed is lower, > 23 (they feed on larger prey), but maximum values extend obliquely with increased turbulence down to prey densities > 10 prey l^{-1}. At 9–10 mm, haddock larvae have an optimum feeding ratio of 18 with a response range similar to the 7–8 mm larvae. Based on these surfaces, turbulence values higher than 10^{-10} W kg^{-1} would lower maximum feeding success dramatically. At intermediate levels of turbulence, feeding success appears to decline with increasing prey density.

Cod has a similar response to haddock, except that the highest feeding ratio for all three size classes occurs at the highest prey densities and generally lower turbulence levels. There is no clearly defined optimum for cod larvae over the same range of conditions as observed for the 7–8 mm and 9–10 mm haddock.

Vertical profiles of larvae and prey in relation to feeding ratio, turbulence, and estimated ingestion rates

MOCNESS tow 189 on Site 81-I, 29 April 1981, provides an example of high wind stress (11.2 m s^{-1}) acting on a non-stratified water column (Fig. 8). Estimated turbulence was 2.5×10^{-6} W kg^{-1} near the surface decreasing to a minimum of 1.3×10^{-9} W kg^{-1} at 25 m depth, increasing again towards the bottom. Larval cod maximum densities were centered at 25 m, the minimum turbulence depth; however, their respective prey densities were low (< 2 prey l^{-1}) at the surface (5 m), increasing with depth to a high (13 prey l^{-1}) at 45 m and deeper. Feeding ratios for 5–6 mm larvae were relatively high (8–10) at mid-depth (25 and 45 m) where most of the larvae occurred, but low (< 4) near surface and at depth. For the 7–8 and 9–10 mm larvae, feeding ratios were in the range of 5–16, but the small sample size precludes establishing a trend with depth. A comparison of feeding ratios with estimated

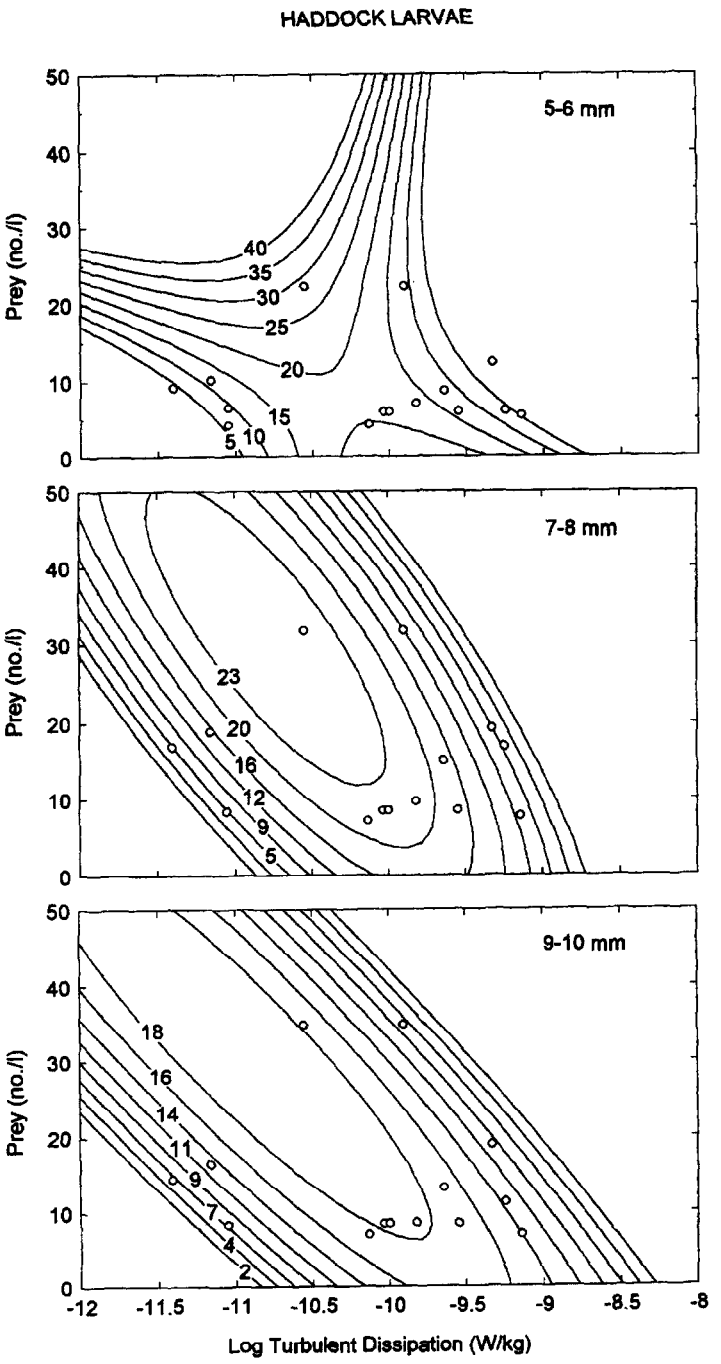

Fig. 7. Response surface estimation of feeding ratio (mean no. prey larva^{-1}) for three size classes of haddock larvae at average prey densities and minimum turbulence levels observed in the upper 50 m of the water column. Actual data points are shown as small circles.

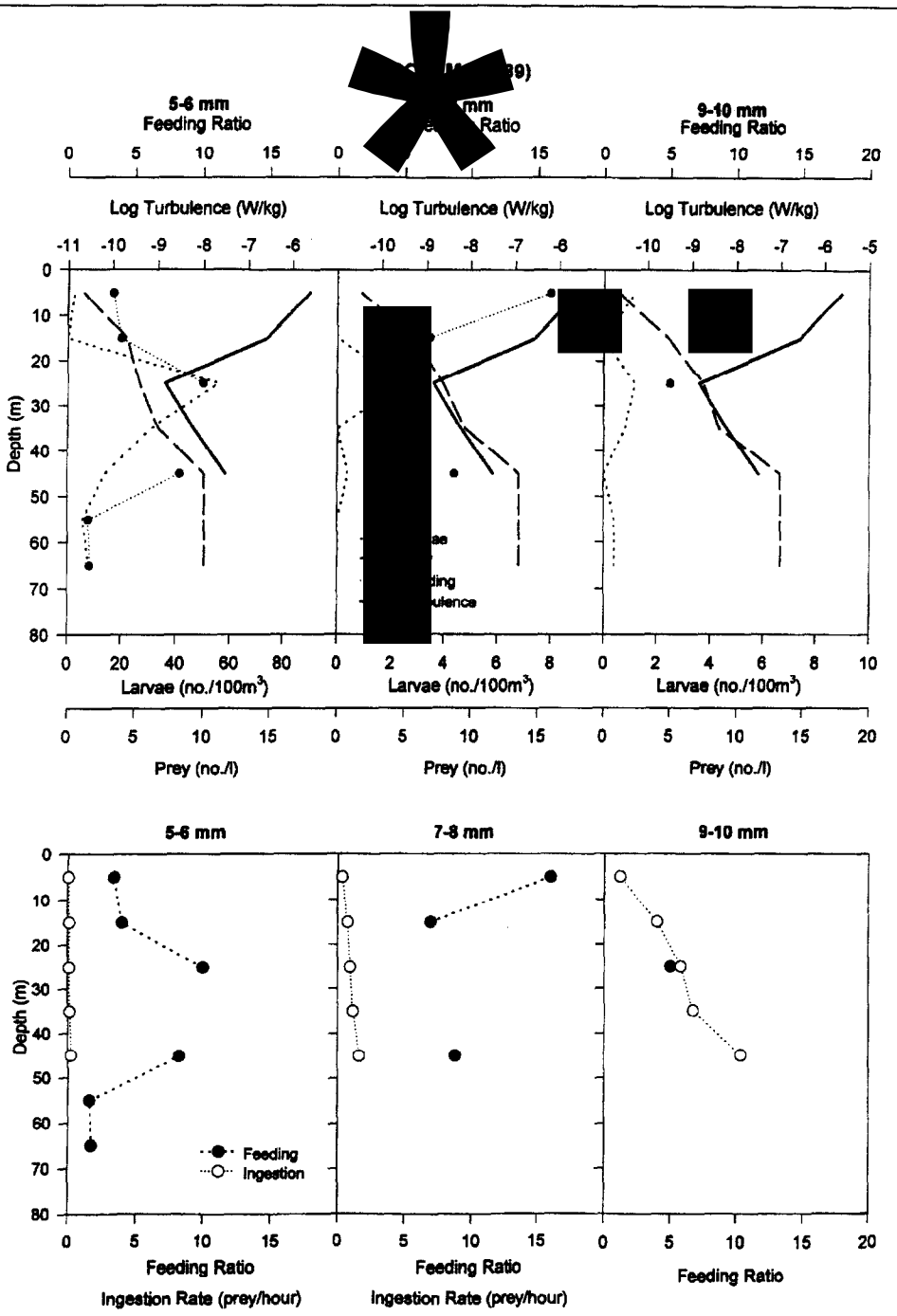

Fig. 8. Vertical distribution of three size classes of cod larvae and their prey in relation to feeding ratio and turbulent dissipation from MOCNESS tow 189 in a non-stratified water column with high-wind (11.2 m s^{-1}) during the previous 5 h. Haul date: 29 April 1981, 15:39–16:03 E.S.T. Lower panels show a comparison of the feeding ratio with an estimated ingestion rate (prey h^{-1}) for a low-speed swimming larva using the Rothschild–Osborn encounter rate model.

ingestion rates also is shown in Fig. 8. Only ingestion rates estimated with the low swim-speed values are shown since the high swim-speed estimates were usually much greater than the observed feeding ratios and not comparable. The estimated hourly ingestion rates should be smaller than the feeding ratio by a factor of 4 if one assumes that gut evacuation time is about 4 h. For MOCNESS 189, the ratio of feeding ratio/ingestion rate is approximately in this range where there are sufficient data, but their depth profiles do not parallel each other.

MOCNESS tow 199 on Site 81-II, 25 May 1981, is an example of low wind stress ($0.8\ m\ s^{-1}$) on a non-stratified water column (Fig. 9). This site was strongly stratified on 21 May 1981 (MOCNESS 191) and then the water column was throughly mixed by an intense storm (Lough, 1984). On 25 May, the near-surface (< 15 m) turbulence level was the lowest estimated ($4.0 \times 10^{-12}\ W\ kg^{-1}$) for any tow. Turbulence increased with depth below 15 m. The 5–6 mm larvae were aggregated at 25 m depth; the 7–8 mm larvae were broadly distributed from surface to 60 m; and the 9–10 mm larvae also were distributed broadly with a maximum density at 35 m. Prey densities ranged from 4 to $26\ l^{-1}$, with irregular peak densities near the surface, mid-depth, and near bottom. Feeding ratios for the 5–6 mm larvae were fairly uniform (4–8) throughout the water column. The 7–8 mm and 9–10 mm larvae, however, had a wide range of feeding ratios (4–16) from surface to near bottom. A comparison of larval feeding ratios with estimated ingestion rates (Fig. 9) shows a similar trend with depth if one allows for displacement due to vertical migration of the larger larvae. Lough and Potter (1993, p. 285) found a significant depth × time interaction effect for cod larvae in an ANOVA of this set of tows, indicating the population centers are located deeper in the water column by day and shoaler by night.

At stratified Site 83-I on 14 May 1993, the following MOCNESS tows 421, 423, and 426 provide a time series from early morning (06:43–07:17 D.S.T.) to noon (12:42–13:07) and evening (18:49–19:19) when the wind increased from 3 to 6–7 $m\ s^{-1}$ (Figs 10–12). A detailed analysis of these tows on the larval vertical distribution in relation to the thermocline is given in Lough and Potter (1993, p. 287). While only haddock is presented here, the same general observations were true for cod.

The 5–6 mm haddock (Fig. 10) were distributed mostly within or above the thermocline or the minimum turbulence region between 15 and 30 m depth. When the wind increased from early morning to noon by a factor of two, the near-surface turbulence estimate also increased 2–3 orders of magnitude, from 7.9×10^{-10} to $1 \times 10^{-7}\ W\ kg^{-1}$. However, at 25 m the minimum turbulence only increased by about 1 order of magnitude, from 1×10^{-11} to $1.6 \times 10^{-10}\ W\ kg^{-1}$. Prey densities were highest near surface (9–20 prey l^{-1}) and relatively low (< 5 prey l^{-1}) deeper than 20 m. The few observations of larval feeding ratios indicated relatively low values (< 7) for the early morning tow (MOCNESS 421), but high values (23 and 38) for the noon and evening tows (MOCNESS 423 and 426, respectively). Low feeding ratios (< 9) were observed for samples deeper than 30 m. The estimated ingestion rates were all < 1, increasing in the surface 20 m similar to the feeding ratios, but greatly underestimating the feeding ratios, based on a 4-h gut evacuation assumption, for the noon and evening tows.

The 7–8 mm haddock larvae (Fig. 11) were distributed broadly in the water column, but most were located within the thermocline (15–30 m), or region of minimum turbulence near 25 m. Prey densities in the early morning tow (MOCNESS 421) were 13–18 prey l^{-1} in the upper 20 m and < 5 prey l^{-1} at deeper depths. By the noon and evening tows (MOCNESS 423, 426), prey density was very high (29 prey l^{-1}) in the surface 10 m, but relatively low

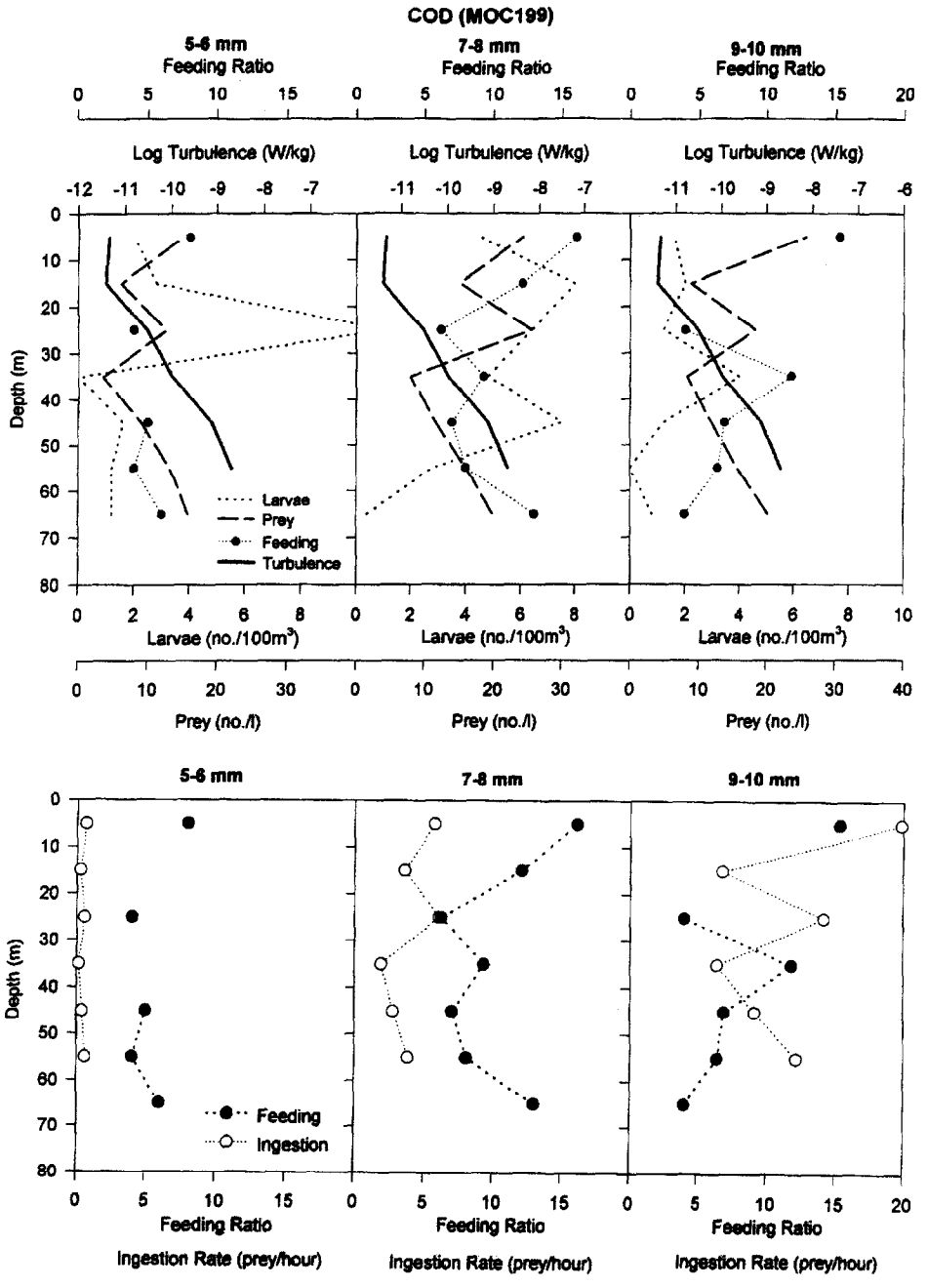

Fig. 9. Vertical distribution of three size classes of cod larvae and their prey in relation to feeding ratio and turbulent dissipation from MOCNESS tow 199 in a non-stratified water column with low-wind (0.8 m s^{-1}) during the previous 5 h. Haul date: 25 May 1981, 13:11–13:41 D.S.T. Lower panels show a comparison of the feeding ratio with an estimated ingestion rate (prey h^{-1}) for a low-speed swimming larva using the Rothschild–Osborn encounter rate model.

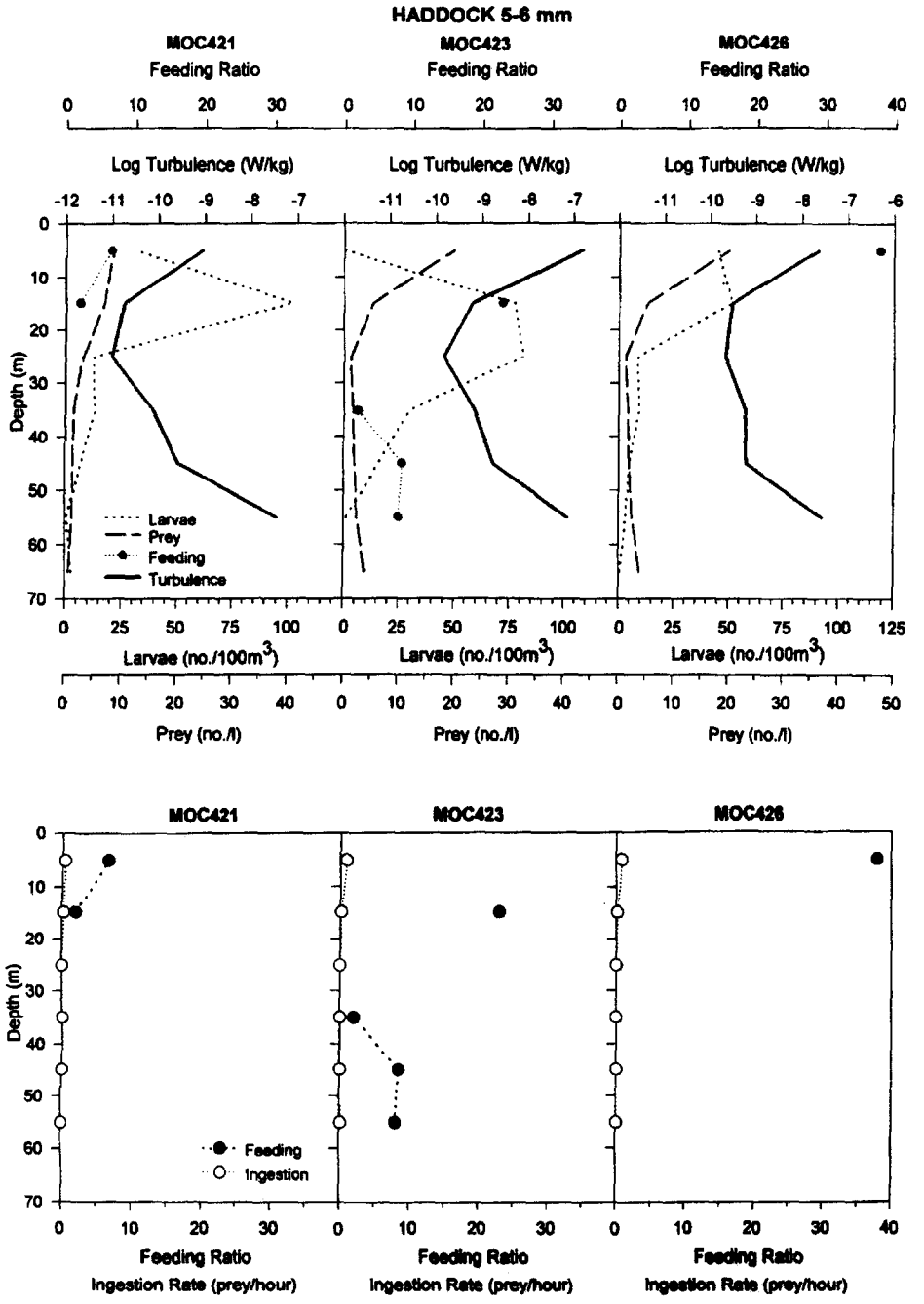

Fig. 10. Vertical distribution of 5–6 mm haddock larvae and their prey in relation to feeding ratio and turbulent dissipation in a stratified water column on 14 May 1983 during three sampling periods: MOCNESS 421, 06:43–07:17 D.S.T., wind speed 3.1 m s^{-1}; MOCNESS 423, 12:42–13:07 D.S.T., wind speed 7.1 m s^{-1}; MOCNESS 426, 18:49–19:19 D.S.T., wind speed 6.0 m s^{-1}. Lower panels show a comparison of the feeding ratio with an estimated ingestion rate (prey h^{-1}) for a low-speed swimming larva using the Rothschild–Osborn encounter rate model.

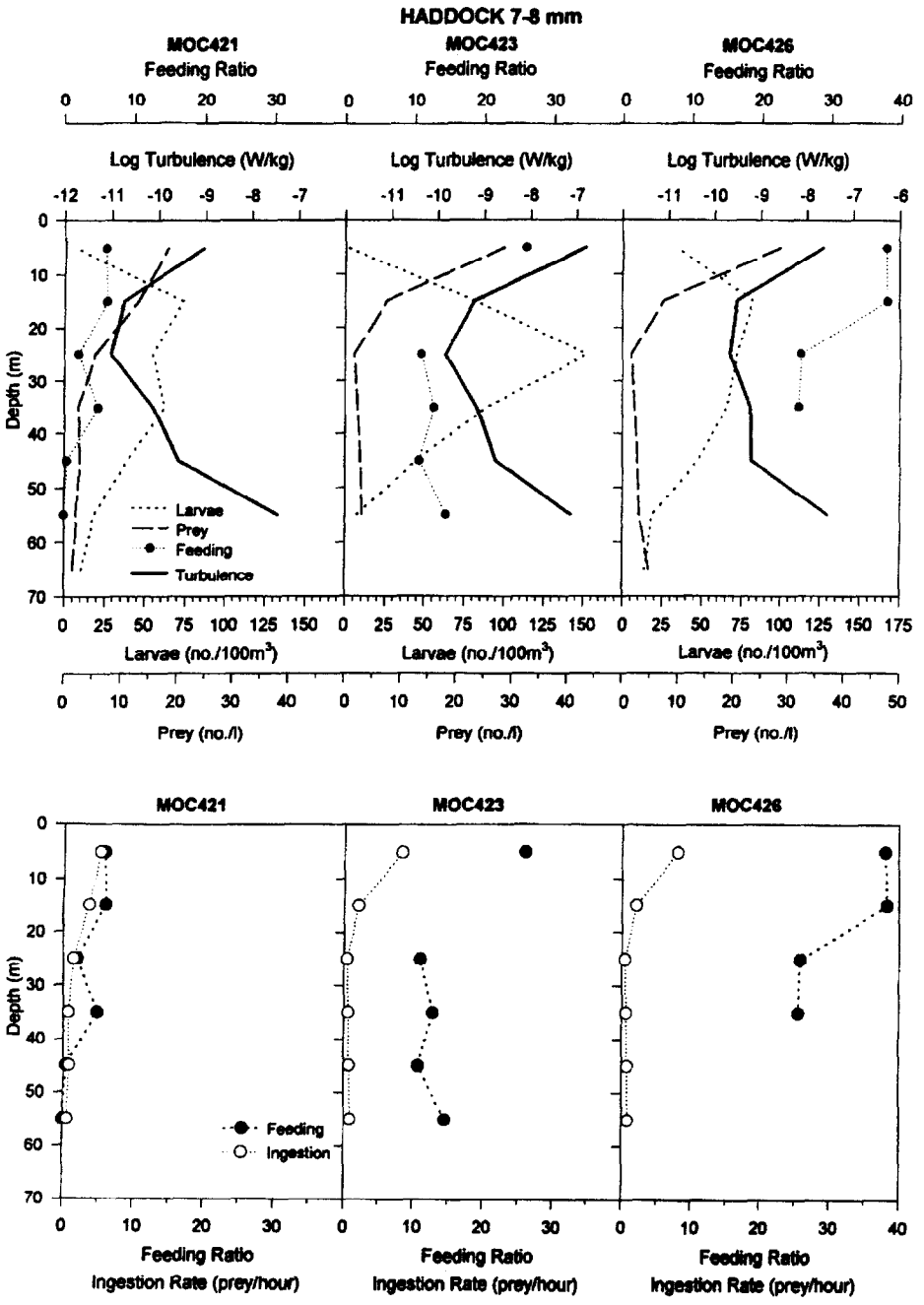

Fig. 11. Vertical distribution of 7–8 mm haddock larvae and their prey in relation to feeding ratio and turbulent dissipation in a stratified water column on 14 May 1983 during three sampling periods: MOCNESS 421, 06:43–07:17 D.S.T., wind speed 3.1 m s^{-1}; MOCNESS 423, 12:42–13:07 D.S.T., wind speed 7.1 m s^{-1}; MOCNESS 426, 18:49–19:19 D.S.T., wind speed 6.0 m s^{-1}. Lower panels show a comparison of the feeding ratio with an estimated ingestion rate (prey h^{-1}) for a low-speed swimming larva using the Rothschild–Osborn encounter rate model.

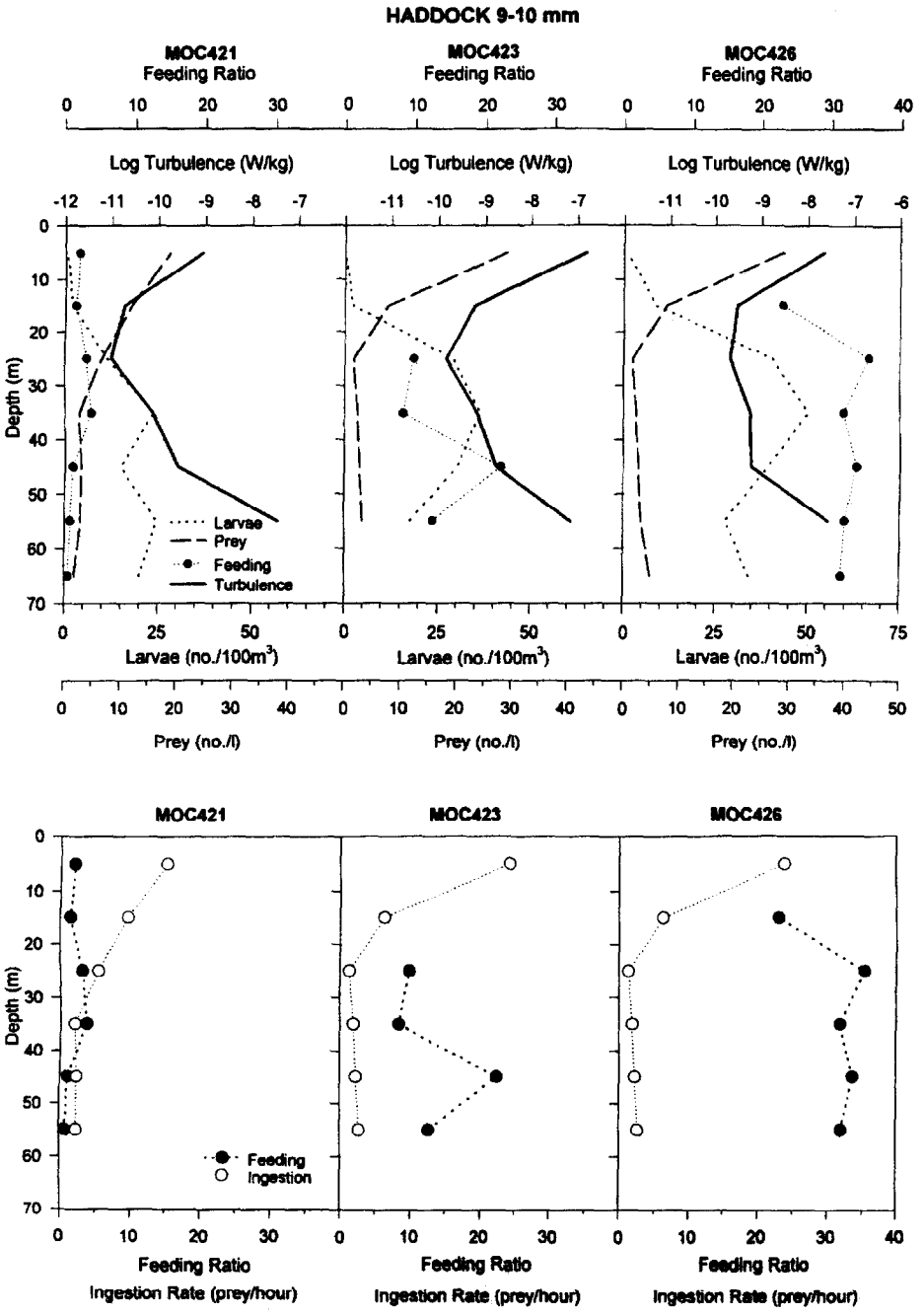

Fig. 12. Vertical distribution of 9–10 mm haddock larvae and their prey in relation to feeding ratio and turbulent dissipation in a stratified water column on 14 May 1983 during three sampling periods: MOCNESS 421, 06:43–07:17 D.S.T., wind speed 3.1 m s^{-1}; MOCNESS 423, 12:42–13:07 D.S.T., wind speed 7.1 m s^{-1}; MOCNESS 426, 18:49–19:19 D.S.T., wind speed 6.0 m s^{-1}. Lower panels show a comparison of the feeding ratio with an estimated ingestion rate (prey h^{-1}) for a low-speed swimming larva using the Rothschild–Osborn encounter rate model.

(<7 prey l^{-1}) throughout the rest of the water column. Larval feeding ratios were considerably higher (25–38) by a factor of 4–8 in the noon and evening tows than early morning. Feeding ratios generally were higher near surface where prey densities also were high. The comparison of estimated ingestion rates with feeding ratios in Fig. 11 shows a similar trend with depth; high near the surface decreasing with depth. The ratio of the two parameters (feeding ratio/ingestion rate) is somewhat greater than 1 for the early morning tow (MOCNESS 421). The noon and evening tows (MOCNESS 423, 426) have ratios much greater than 1; however, their surface ratios are in the range 3–5, which is in close agreement with the 4-h gut evacuation time.

The 9–10 mm haddock larvae (Fig. 12) were found mostly below 20 m in the day tows with maximum densities at 35 m depth, the base of the thermocline. This size of larvae was found by Lough and Potter (1993) to migrate vertically. About 60% of the larvae were found below the thermocline by day, but 80% were found within or above the thermocline at night. Prey density profiles were similar to those for the smaller size classes of larvae (Figs 10 and 11), relatively high near the surface and low throughout the water column. The near surface prey density increased from 19 prey l^{-1} in the early morning tow (MOCNESS 421) to 29 prey l^{-1} during the noon and evening tows (MOCNESS 423, 426). Too few larvae were caught in the upper 20 m for feeding ratios to be reliable at these depth levels. Feeding ratios for larvae caught where most of the day population resided were low (1–4) from the early morning tow but were higher (8–35) from the noon and evening tows. The estimated ingestion rates do not track with feeding ratios in the upper 20 m, but at deeper depths the early morning tow had feeding ratios/ingestion rates near 1; the noon tow ratios were in the range of 4–10; and the evening tow ratios, 12–27. Because these larger larvae vertically migrate in a day–night cycle, they could be feeding to some degree higher in the water column than where they were caught during the early morning tow (MOCNESS 421) as they descend from the surface. In contrast, they may be feeding at deeper depths than where they were caught in the evening haul (MOCNESS 426) as they migrate upwards near sunset. Therefore, in some cases it may not be possible to precisely match estimated ingestion rates with feeding ratios at specific depth levels.

DISCUSSION

Rothschild and Osborn (1988) proposed increased contact rate between a planktonic predator and its prey due to turbulence. Previous applications of this theory to larval observations (Sundby and Fossum, 1990; MacKenzie and Leggett, 1991, 1993) did not consider the vertical profile of the turbulence-induced contact rate in stratified water columns. That vertical profile was estimated in this analysis using the one-dimensional, mixed-layer model of James (1977). Estimating the vertical profile of turbulent dissipation from standard measurements of temperature, salinity and local wind speed is inexact, at best. However, the method is believed to provide a dynamically-based, consistent approach for using the large larval data set to evaluate the effect of turbulence on larval feeding in stratified water columns. The estimated turbulence values generally are comparable to or less (1–2 orders of magnitude) than those values observed along the northern flank of Georges Bank (48–63 m bottom depth) by Horne *et al.* (1996). The calculated turbulence values could be increased with a different choice of the σ and p parameters; however, these parameters were chosen on the basis of a best fit to a 11-year data base for thermocline development on the southern flank of Georges Bank (Appendix). Despite the uncertainty of

the absolute values, the relative change in turbulent intensity through the water column remains independent of the parameter choice.

The data analyses employed rely on the assumptions that wind-mixing of the surface layer has been of sufficient duration and is representative of conditions over the previous 5 h for larval feeding, and that the prey densities sampled by the 1/4-m^2 MOCNESS represent those experienced by the larvae during this time, assuming a 4-h gut evacuation rate on average for the feeding ratio. Sampled volumes for larvae were on the order of 250 m^3 and for their prey about 25 m^3, with a vertical resolution of 10 m. These relatively large sampled volumes over 10-m strata could average out any smaller-scale patchiness that may have been present, especially higher densities of prey in more vertically stratified waters, and contribute to the high variance in the data. High densities of copepod nauplii (40–160 l^{-1}) were found by Incze *et al.* (1996) in stratified waters, generally at 20–10 m depth, on the southern flank of Georges Bank in May 1992 using a plankton pump with about 5-m vertical resolution. Also, the microzooplankton component of first-feeding larvae was not adequately addressed in our study. Recent ship-board experiments by Gallagher *et al.* (1996), using first-feeding cod larvae, found that protozoans were ingested exclusively during yolk-sac absorption. Special techniques are needed to resolve the rapidly digested protozoans. Only after yolk-sac absorption were larvae developed sufficiently to feed on copepod nauplii.

In the response surface analyses, there was no relationship between depth-specific feeding ratios and density of prey; however, there was a negative relationship between depth-averaged (50 m) feeding ratios and mean prey density, and a minimum water-column turbulence estimate. Due to the interaction effect of prey density and turbulence, the maximum feeding ratio decreases with increasing prey density from low to intermediate levels of turbulence (Fig. 7). This could be an artifact of the model fitting, insufficient data to resolve this region, or a behavioral response of the larva where higher densities of prey in motion cause a distraction to the pursuit and capture process. Maximum feeding ratios also declined rapidly at turbulence values above 10^{-10} W kg^{-1} at all prey densities. At these higher turbulence levels, which represent a *minimum* index of the water column, turbulence may simply overwhelm the larva's attempt to ingest prey. Also, bear in mind that the estimated turbulence estimates may be 1–2 orders of magnitude lower compared to other studies. Without regard to absolute values, the response surfaces indicate that recently-hatched larvae (5–6 mm) have the highest feeding ratios at the higher densities of prey and lower turbulence levels. Older larvae (7–8, 9–10 mm) have maximum feeding ratios also at high prey densities and low turbulence, but the maximum ratios extend to lower prey levels at intermediate levels of turbulence, presumbably as a result of the increased contact rate.

An index of larval feeding activity was represented by a feeding ratio, the mean number of prey per larval gut, from field collected specimens; however, larval gut fillings and evacuation rates are dependent upon multiple factors, which include larval size, prey availability, state of digestion, temperature, and light (Tilseth and Ellertsen, 1984). In their laboratory studies of first-feeding cod larvae, digestion of a copepod nauplius ranged from 30 min to 1 h 30 min. The passage of prey through the gut varied with temperature and volume of prey in the gut. When prey were available continuously, larvae would fill their gut within 3 h and started gut evacuation after gut filling reached a maximum level. For older larvae just beyond first-feeding, the gut contents probably represent feeding from the previous 4 h, on average, but depending on conditions it may range 1–9 h. Fortier and Harris (1989) in their study of foraging of fish larvae used a constant 3.2 gut fillings for a 14-h feeding period, which would amount to a gut evacuation rate of once every 4.4 h.

Regardless of the exact gut evacuation rate, a 4-h period was used only as a guide in this study to compare the possible offset of depth-specific larval feeding ratios with estimated ingested rates. The challenge is to explain differences between the observed and estimated values.

In our Georges Bank study the maximum feeding ratios were generally in the range of 20–30 prey larva^{-1}, but as high as 38 for the smallest size class, 5–6 mm larvae (Table 5, Figs 5 and 6). Sundby and Fossum (1990) and Sundby *et al.* (1994) in studies of Arcto-Norwegian first-feeding cod larvae, 8–10 days old, found comparatively low feeding ratios <3–6, whereas the averaged naupliar densities were similar to that observed in our Georges Bank study of less than 50 prey l^{-1}. The diet of first-feeding Arcto-Norwegian cod is 95% nauplii of *Calanus finmarchicus*, whereas the Georges Bank larvae feed on a diversity of small nauplii and copepodites of primarily *Pseudocalanus* spp. and *Oithona* sp. Biasing of results due to gut evacuation and regurgitation in the net generally is not as big a problem for the coiled-gut gadids as it is for the straight-gut herring. And similar feeding ratios were reported from vertical net hauls (Sundby and Fossum, 1990) and plankton pump sampling (Sundby *et al.*, 1994). Perhaps, in terms of volume or biomass, the larger *Calanus* prey only available for the Arcto-Norwegian cod larvae would equal the smaller prey selected in the Georges Bank study.

Other investigators have noted that feeding ratios for cod and haddock larvae have increased during the day to a peak just before sunset (Kane, 1984; Sundby *et al.*, 1994). This same phenomenon was observed in the present study for each of the three size classes observed in the series of tows from early morning (MOCNESS 421) to noon (MOCNESS 423) and evening (MOCNESS 426) (Figs 10–12). Compared to the low early morning feeding ratios, they increased by a factor of 2–6 by noon, and 7–13 by evening, the larger larvae showing the greater increase (Table 5). This increased feeding ratio may be partly explained by the increased turbulence caused by the wind speed increasing from 3 m s^{-1} in early morning to 6–7 m s^{-1} by afternoon, leading to increased contact rates between larvae and their prey. However, the modeled estimated ingestion rates only increased significantly in the upper 20 m where prey density was highest, whereas larvae throughout the entire water column had elevated feeding ratios. The 5–6 mm and 7–8 mm larvae do not migrate any significant distance vertically, so that another behavioral factor may be involved such as an optimum light intensity. Ellertsen *et al.* (1980) found first-feeding cod larvae to have a light intensity threshold between 0.1–0.4 lux. The highest feeding intensity was observed at 1.4 lux. Laboratory experiments conducted by Skiftesvik (1994) on larval cod kept at different light intensities showed that light level can affect their metabolism, swimming and feeding activity, vertical distribution, morphology, and mortality. Light measurements from field studies should be incorporated into these feeding studies.

The mean length of prey ingested for each larval size class was chosen for estimating its cruising speed as opposed to incorporating an ensemble of prey sizes. The two most important prey items could be grouped as copepod nauplii and copepodites. On average, one could designate the length of the nauplii as 200 μm and the copepodite stage as 400 μm. Then their respective cruising speeds would be 0.01 cm s^{-1} and 0.02 cm s^{-1}. Since Sundby's (1995) study found that the relative contact rates were insensitive to prey swimming speed, we felt it was appropiate to use just the overall mean prey length for a larval size class. However, in future work with larger larvae and juvenile fish, adding an ensemble of prey swimming speeds would add another dimension of realism to the simulations.

MacKenzie *et al.* (1994) hypothesized that in a highly turbulent environment, larvae may

switch to selecting more vulnerable prey where pursuit times are shorter. This may explain why a large fraction of the larval cod and haddock diet is composed of copepod nauplii, even as larger larvae. Haddock larvae consistently appear to select smaller prey than cod, which may reflect differences in pursuit behavior. Also, consistent with this hypothesis is the finding that 28% of the 5–6 mm haddock larvae contained phytoplankton, whereas only 7.6% of the 5–6 mm cod larval guts contained phytoplankton. Recent laboratory studies have demonstrated that cod larvae should be considered as pause–travel predators, searching for prey after a short swimming period (Skiftesvik, 1994). Using a pause–travel encounter model based on experimental results for 5–6 mm larval cod, MacKenzie and Kiørboe (1995) found that prey contact rates increased at high turbulence by a factor of 5 compared to a cruise model.

There is not yet sufficient laboratory data to more accurately parameterize behavior of the different sizes of larvae used in our study. Nevertheless, the use of average swimming speeds (low estimate) appears to provide reasonable comparisons between observed larval feeding ratios and estimated ingestion rates. The best correspondence was with the 7–8 mm larvae, which simply may be due to the fact that more larvae were available for estimating mean feeding ratios at discrete depths than for the other size classes. The low swimming speed used may be over-estimating the ingestion rate for the 5–6 mm larvae and under-estimating the ingestion rate for the 9–10 mm larvae. Or, differences between the estimated and observed values may reflect differential digestion time, or gut evacuation time for the small and large larvae. The 9–10 mm larvae have the confounding effect of extensive vertical migration, which, depending on the time of day, may not allow direct vertical comparisons. This calls for the use of selective water-column averaging of the important parameters.

The question still remains on the relative importance of mixing versus stratification on the feeding process. It seems intuitive that an optimum level exists where stratification can aggregate prey while mixing at moderate levels can increase the probability of contacts between larvae and their prey. At higher levels of turbulence the enhancement of contact rates may be negated by the interruption of the pursuit process, resulting in a lower ingestion rate. In nature, there is probably an optimum balance between the processes of mixing and stratification which results in maximum feeding, growth and survival of larvae. By residing near the pycnocline where there is a sharp gradient in turbulence, larvae have a greater probability of encountering optimum feeding conditions within a short distance vertically, especially first-feeding larvae with limited swimming ability.

Acknowledgements—This is contribution 48 of the U.S. GLOBEC program, funded jointly by NOAA and NSF. We thank T. Rotunno and E. Broughton for their help in the production of tables and plots, and B. MacKenzie for his review of the manuscript.

REFERENCES

Alderdice D. F. (1972) Factor combinations. Responses of marine poikilotherms to environmental factors acting in concert. In: *Marine ecology*, Vol. 1, Part 3, O. Kinne, editor, Wiley-Interscience, London, pp. 1659–1722.

Auditore P. J. (1984) Stomach content analysis, processing methods for larval gadids. NMFS/NEFC Woods Hole Laboratory Reference Document Number 84–14, 48 pp.

Bolz G. R. and R. G. Lough (1983) Growth of Atlantic cod, *Gadus morhua*, and haddock, *Melanogrammus aeglefinus*, on Georges Bank, spring 1981. *Fishery Bulletin, U.S.*, **81**, 826–827.

Bolz G. R. and R. G. Lough (1988) Growth through the first six months of Atlantic cod, *Gadus morhua*, and haddock, *Melanogrammus aeglefinus*, based on daily otolith increments. *Fishery Bulletin, U.S.*, **86**, 223–235.

Buckley L. J. and R. G. Lough (1987) Recent growth, biochemical composition, and prey field of larval haddock

(*Melanogrammus aeglefinus*) and Atlantic cod (*Gadus morhua*) on Georges Bank. *Canadian Journal of Fisheries and Aquatic Sciences*, **44**, 14–25.

Corkett C. J. and I. A. McLaren (1978) The biology of *Pseudocalanus*. *Advances In Marine Biology*, **15**, 1–231.

Davis C. S., G. R. Flierl, P. H. Wiebe and P. J. S. Franks (1991) Micropatchiness, turbulence and recruitment in plankton. *Journal of Marine Research*, **49**, 109–151.

Ellertsen B., P. Solemdal, T. Strømme, S. Tilseth, T. Westgard, E. Moksness and V. Øiestad (1980) Some biological aspects of cod larvae (*Gadus morhua* L.). *Fiskeridirektoratets Skrifter Serie Havundersøkelser*, **17**, 29–47.

Fortier L. and R. P. Harris (1989) Optimal foraging and density-dependent competition in marine fish larvae. *Marine Ecology Progress Series*, **51**, 19–33.

Gallagher S. M., I. Von Herbing, and L. Davis (1996) Yolk-sac cod larvae ingest microzooplankton exclusively from natural plankton assemblages on Georges Bank. EOS Abstract, AGU/ASLO Meeting, San Diego, CA, 12–15 February 1996.

Horne E. P. W., J. W. Loder, C. E. Naimie and N. S. Oakey (1996) Turbulent dissipation rates and nitrate supply in the upper water column on Georges Bank. *Deep-Sea Research II*, **43**, 1683–1712.

Hunter J. R. (1981) Feeding ecology and predation of marine fish larvae. In: *Marine fish larvae*, R. Lasker, editor, University of Washington Press, Seattle, pp. 34–77.

Incze L., P. Aas and T. Ainaine (1996) Distribution of copepod nauplii and turbulence on the southern flank of Georges Bank: implications for feeding by larval cod (*Gadus morhua*). *Deep-Sea Research II*, **43**, 1855–1873.

James I. D. (1977) A model of the annual cycle of temperture in a frontal region of the Celtic Sea. *Estuarine and Coastal Marine Science*, **5**, 339–353.

Kane J. (1984) The feeding habits of co-occurring cod and haddock larvae from Georges Bank. *Marine Ecology Progress Series*, **16**, 9–20.

Laurence G. C. (1985) A report on the development of stochastic models of food limited growth and survival of cod and haddock larvae. In: *Growth and survival of larval fishes in relation to the trophodynamics of Georges Bank cod and haddock*, G. C. Laurence and R. G. Lough, editors, NOAA Technical Memorandum NMFSS-F/NEC-36, Woods Hole, MA, pp. 83–150.

Lough R. G. (1984) Larval fish trophodynamic studies on Georges Bank: sampling strategy and inital results. In: *The propagation of cod* Gadus morhua *L.*, E. Dahl, D. S. Danielssen, E. Moksness and P. Solemdal, editors, Flødevigen rapportser, 1, pp. 395–434.

Lough R. G. and G. R. Bolz (1989) The movement of cod and haddock onto the shoals of Georges Bank. *Journal of Fish Biology*, **35**, 71–79.

Lough R. G. and D. C. Potter (1983a) Rapid shipboard identification and enumeration of zooplankton samples. *Journal of Plankton Research*, **5**, 775–782.

Lough R. G. and D. C. Potter (1993b) Vertical distribution patterns and diel migrations of larval and juvenile haddock *Melanogrammus aeglefinus* and Atlantic cod *Gadus morhua*. *Fishery Bulletin, U.S.*, **91**, 281–303.

MacKenzie B. R. and T. Kiorboe (1995) Encounter rates and swimming behavior or pause–travel and cruise larval fish predators in calm and turbulent laboratory environments. *Limnology and Oceanography*, **40**, 1278–1289.

MacKenzie B. R. and W. C. Leggett (1991) Quantifying the contribution of small-scale turbulence to the encounter rates between larval fish and their zooplankton prey: effects of wind and tide. *Marine Ecology Progress Series*, **73**, 149–160.

MacKenzie B. R. and W. C. Leggett (1993) Wind-based models for estimating the dissipation rates of turbulent energy in aquatic environments: empirical comparisons. *Marine Ecology Progress Series*, **94**, 207–216.

MacKenzie B. R., T. J. Miller, S. Cyr and W. C. Leggett (1994) Evidence for a dome-shaped relationship between turbulence and larval fish ingestion rates. *Limnology and Oceanography*, **39**, 1790–1799.

Miller T. J., L. B. Crowder, J. A. Rice and E. A. Marschall (1988) Larval size and recruitment mechanisms in fishes: towards a conceptual framework. *Canadian Journal of Fisheries and Aquatic Science*, **45**, 1657–1670.

Rothschild B. J. and T. R. Osborn (1988) Small-scale turbulence and plankton contact rates. *Journal of Plankton Research*, **10**, 465–474.

Skiftesvik A. B. (1994) Impact of the physical environment of the behaviour of cod larvae. *ICES Marine Science Symposium*, **198**, 646–653.

Skiftesvik A. B. and I. Huse (1987) Behaviour studies of cod larvae, *Gadus morhua* L. *Sarsia*, **72**, 367–368.

Statsoft (1991) CSS (Complete Statistical System): STATISTICA. *Vol. II, Non-linear estimation*, Tulsa, OK, pp. 423–462.

Sundby S. (1995) Wind climate and foraging of larval and juvenile Arcto-Norwegian cod (*Gadus morhua* L.). *Canadian Special Publication of Journal of Fisheries and Aquatic Science*, **121**, 405–415.

Sundby S. and P. Fossum (1990) Feeding conditions of Arcto-Norwegian cod larvae compared with the Rothschild–Osborn theory on small-scale turbulence and plankton contact rates. *Journal of Plankton Research*, **12**, 1153–1162.

Sundby S., B. Ellertsen and P. Fossum (1994) Encounter rates between first-feeding cod larvae and their prey during moderate to strong turbulent mixing. *ICES Marine Science Symposium*, **198**, 393–405.

Tilseth S. and B. Ellertsen (1984) Food consumption rate and evacuation processes of first feeding cod larvae (*Gadus morhua* L.). In: *The propagation of cod* Gadus morhua *L.*, E. Dahl, D. S. Danielssen, E. Moksness and P. Solemdal, editors, Flødevigen rapportser 1, pp. 167–182.

Turner J. S. (1981) Small-scale mixing processes. In: *Evolution of physical oceanography*, B. A. Warren and C. Wunsch, editors, MIT Press, Cambridge, MA, pp. 236–263.

Wiebe P. H., A. W. Morton, A. M. Bradley, R. H. Backus, J. E. Craddock, V. Barber, T. J. Cowles and G. R. Flierl (1985) New developments in the MOCNESS, an apparatus for sampling zooplankton and micronekton. *Marine Biology*, **87**, 313–323.

APPENDIX

To estimate the increase in contact rate between a planktonic predator and its prey due to turbulence (Rothschild and Osborn, 1988), an estimate of the turbulent dissipation is needed. Turbulent dissipation rate ε can be parameterized in terms of the vertical shear of the mean current U through use of an eddy coefficient K (Turner, 1981, eqns 8.3 and 8.4):

$$\varepsilon = K(\mathrm{d}U/\mathrm{d}z)^2.$$

To estimate the vertical profile of the eddy viscosity and the mean current shear, the formulation presented by James (1977) is used. The vertical shear is determined by:

$$\left(\frac{\partial U}{\partial z}\right)^2 = \frac{1}{2}\left(\frac{A}{h-z}\right)^2 + \frac{B^2}{z^2}$$

where h is the water depth, z is depth from the surface, $A = W^*/k$, $B = w^*/k$ and k is von Karman's constant = 0.41. W^* is the friction velocity due to the tide and w^* the friction velocity due to the wind:

$$W^* = C^{\frac{1}{2}}V,$$

$$w^* = \left(\frac{\rho_a}{\rho}\right)^{\frac{1}{2}} C_1^{\frac{1}{2}} W,$$

where $C = 0.002$ is the bottom friction coefficient, $C_1 = 0.0025$ is the wind stress coefficient, $\rho_a/\rho = 0.00125$ is the ratio of air to water density, V is the tidal current speed and W is the wind speed.

The eddy viscosity K is parameterized in terms of a gradient Richardson number. It is expressed as the sum of a wind and a tidal component

$$K = A_w + A_t,$$

where

$$A_w = A_{0w}(1 + \sigma Ri)^{-p},$$

$$A_t = A_{0t}(1 + \sigma Ri)^{-p},$$

$$Ri = g\frac{\partial \rho}{\partial z}\left(\frac{\partial U}{\partial z}\right)^{-2},$$

$$A_{0w} = 4.3 \times 10^{-4}\ \mathrm{W^2\ m^2\ s^{-1}} (W > 4.2\ \mathrm{m\ s^{-1}}),$$

$$= 1.02 \times 10^{-4}\ \mathrm{W^3\ m^2\ s^{-1}} (W < 4.2\ \mathrm{m\ s^{-1}}),$$

$$A_{0t} = 1.59 \times 10^{-3}\ \mathrm{V\ h}.$$

Ri is the gradient Richardson number, g is gravity, and σ and p are two free parameters. These parameters were chosen based on the best fit for the seasonal development of the thermocline on the southern flank of Georges Bank using the mean water-column values from the MARMAP 1977–87 data base.